Session 1

Galaxy Building blocks

https://doi.org/10.1017/S1743921306004935 Published online by Cambridge University Press

Galaxy Evolution across the Hubble Time
Proceedings IAU Symposium No. 235, 2006
F. Combes & J. Palouš, eds.

doi:10.1017/S1743921306004935

The Tully-Fisher Relation as a Function of Redshift: Disentangling Galaxy Evolution and Selection Biases

Nicole P. Vogt

Department of Astronomy, New Mexico State University, Las Cruces, NM 88003, USA
email: nicole@nmsu.edu

Abstract. We review the status of current observations of the fundamental parameters of intermediate redshift ($z \leqslant 1.2$) disk galaxies. Advances in instrumentation of 8-10m class telescopes have made possible detailed measurements of galaxy luminosity, morphology, kinematics and mass, in both the optical and the infrared passbands. By studying such well known star formation indicators as [OII]3727A (in the optical) and Hα (redshifted to the infrared), the internal velocity structure and star formation rates of galaxies can be traced through this entire redshift regime. The combination of throughput and optimum seeing conditions yields spectra which can be combined with high resolution multiband imaging to explore the evolution of galaxies of various morphologies, and to place constraints on current models of galaxy formation and star formation histories.

Out to redshifts of unity, these data form a high redshift Tully-Fisher relation that spans four magnitudes and extends to well below L*, with no obvious change in shape or slope with respect to the local relation. A comparison of disk surface brightness between local and high redshift samples yields an offset in accordance with distance-dependent surface brightness selection effects, as can the apparent change in disk size with redshift for disks of a given mass. These results support low Ω_0 models of formation, and provide further evidence for modest increases in luminosity with lookback time for the bulk of the observed field spiral galaxy population.

Finally, a comparison of spatially resolved spectra versus integrated emission line widths for distant galaxies suggests that observational constraints bias each type of observational sample toward different sub-groups of galaxies, with different evolutionary histories. Like varying selection effects, this will lead to a wide range of projected evolutionary trends.

Keywords. galaxies: evolution, galaxies: fundamental parameters, galaxies: spiral, galaxies: formation

1. Introduction

High redshift kinematic studies represent an intriguing technique for probing the evolution of disk galaxies. While imaging samples tend to be quite sensitive to instantaneous star formation and the variability of galaxy luminosity, the kinematic focus upon galaxy mass leads us toward a picture more representative of the long-term evolution of systems.

Kinematic samples are typically sub-samples of general redshift surveys, where objects are re-observed at higher spectral resolution and/or with the spectrograph aligned along or near to the galaxy major axis. Recent complimentary efforts by three research groups (IA Göttingen, U Nottingham, and my DEEP work at NMSU/UCSC) are providing us with a wide range of data, taken with different observational set-ups and utilizing quite different selection criteria in choosing samples of objects. In this talk, I shall describe the effect of a few key selection criteria, and also consider several observational constraints upon velocity measurements.

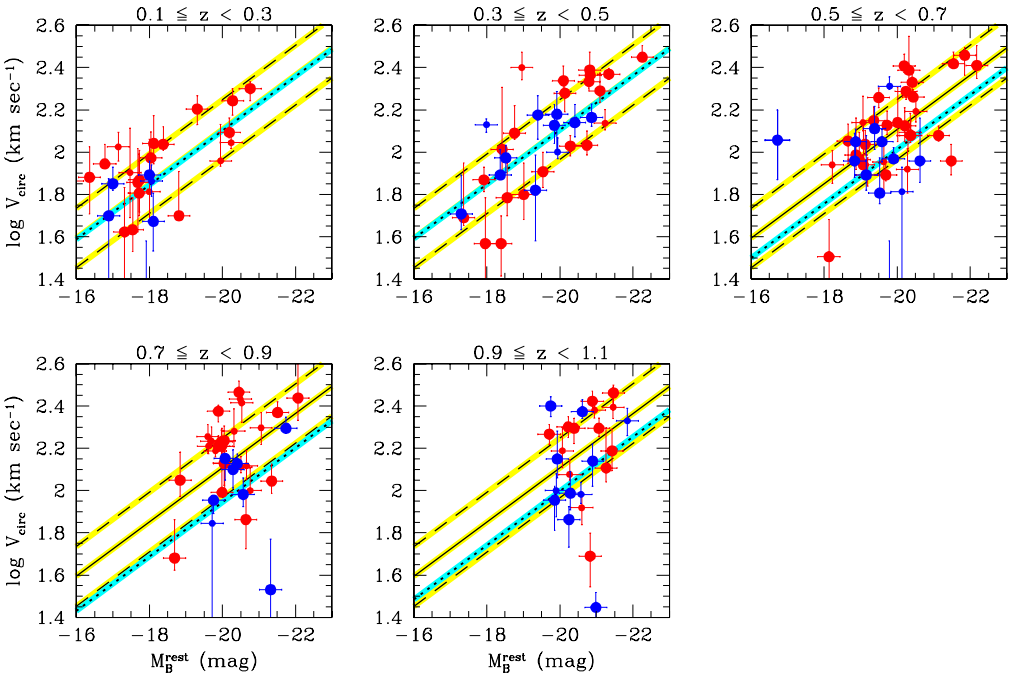

Figure 1. The B-band Tully-Fisher relation, divided into five redshift bins. Yellow solid and dashed lines indicate the local relationship, flanked by $\pm 2\sigma$ lines, while the cyan dotted line indicates the y-offset fit to large equivalent width objects (with strong Hα and [OII]3727 flux, dark blue points) within each bin, shifted out by a full magnitude by $z = 1$.

2. The Effects of Selection Criteria on High Redshift Kinematics

Redshift surveys typically impose magnitude limits upon samples; objects chosen for kinematic follow-up work are then selected by a combination of emission line strength strength, morphology, inclination angle, and position angle on the sky. Kinematic samples may then be further winnowed by examination of emission line strength in a particular feature, the amount of nuclear concentration, or the radial flux extent. The length, and depth, of exposures, and the degree of position angle offsets from galaxy major axis, also play a role in determining which galaxies are retained for further examination, and the quality of derived spatially extended spectral lines.

Various published samples show evidence for evolution in the Tully-Fisher relation from zero to roughly one magnitude in brightening. The primary point we wish to make is that the strength of the observed effect is strongly dependent upon how observed samples are constructed.

Consider the DEEP sample of objects shown in Figure 1. This sample was drawn from a general redshift sample, and slitlets were aligned exactly with galaxy major axis for all elongated objects whose position angles fell within $\pm 30°$ of the field angle on the sky. (Thus roughly 33% of all elongated objects were studied, and in each case the spectrograph slitlet was aligned exactly along the galaxy major axis.) No morphological selection was done beyond the minimum requirement of elongation, sufficient to remove face-on disks and round ellipticals. Early type (e.g., S0) galaxies with absorption of key optical emission lines were deemed unsuccessful targets, but observations were extended for up to ten hours per object on a 10-meter telescope in order to probe emission down

https://doi.org/10.1017/S1743921306004935 Published online by Cambridge University Press

to very faint levels, to guard against removing low equivalent width objects from the sample.

Figure 1 demonstrates how sensitive measured offsets in the Tully-Fisher become to the equivalent width of [OII]3727 flux at redshifts $z \sim 1$. At low redshifts the low and high equivalent width objects occupy the same space, but at redshifts above one-half low equivalent width objects follow the local relation while those with high equivalent widths become brighter and brighter, lying offset by a full magnitude by $z = 1$. As high equivalent width galaxies are the easiest to detect and trace in spectra, they tend to be over-sampled in kinematic surveys. We can substitute nuclear concentration for equivalent width, and find the same trend for high concentration index objects.

We note that a set of objects appear within each redshift bin at the magnitude limit of the parent redshift survey, appearing both along the Tully-Fisher relation and below it. As the magnitude limit propagates to brighter intrinsic magnitudes with increasing redshift, each successive redshift bin fills this pattern with objects of increasing intrinsic brightness. (This produces high surface brightness objects which draw the mean offset away from the local relation, as the magnitude limit is not perpendicular to the Tully-Fisher relation.) Traditional-evolution simulations reproduce this effect in modeled samples, and it is also paralleled by the overall increase in surface brightness with redshift based purely on the sensitivity of the underlying imaging samples.

There are also implicit size requirements that act to bias kinematic samples. One requires an angular extent of ideally $1\farcs5$ or greater, in order to deconvolve the underlying velocity profile from the blurring effects of the seeing disk. For a fixed ratio of the gas radius to the disk scale length, this acts to remove galaxies with small disk scale lengths at high redshifts. If the ratio is allowed to vary (and in fact it is probable that it is evolving along with the growth of the galaxy disks), then this limit acts to remove galaxies with small gas radii (the extent of the emission traced along the disk) from kinematic samples. We also require that the emission line flux extends out to at least 2.5 disk scale lengths along the disk, in order for the derived circular velocity to be representative of the disk at reasonable radii.

Note that because these samples extend further down the luminosity function at lower redshifts, these size effects are as important at low redshifts as they are at the high redshift end of the sample. We are in fact preferentially observing objects with the largest gas radii at redshifts as low as $z = 0.2$. On the positive side, however, it is worth noting that the angular size function increases by only a factor of two between $z = 0.4$ and $z = 1$.

3. Circular Velocities and Integrated Velocity Widths

As spatially resolved velocity profiles are quite difficult to obtain at high redshifts, it is natural to ask how much kinematic information can be derived from integrated profiles, where the spectral flux is collapsed into a single spatial channel.

Figure 2 shows the relationship between circular velocities and integrated velocities, for the sample of DEEP elongated galaxies shown previously in Figure 1. We observe that there is a rough correspondence between measures, even though all spatial information has been removed from the line width measurements. The range of line width appears sightly compressed in velocity space, particularly for low objects with low circular velocities. It is expected that there exists a population of galaxies with integrated line widths for which the full velocity profile cannot be traced, because (1) the galaxy position angle made it impossible to place a slitlet along the major axis or (2) the spectral flux does not extend far enough out along disk. Note, however, that there is also a population of objects for which a rotation curve could be traced which were too faint to meet the

https://doi.org/10.1017/S1743921306004935 Published online by Cambridge University Press

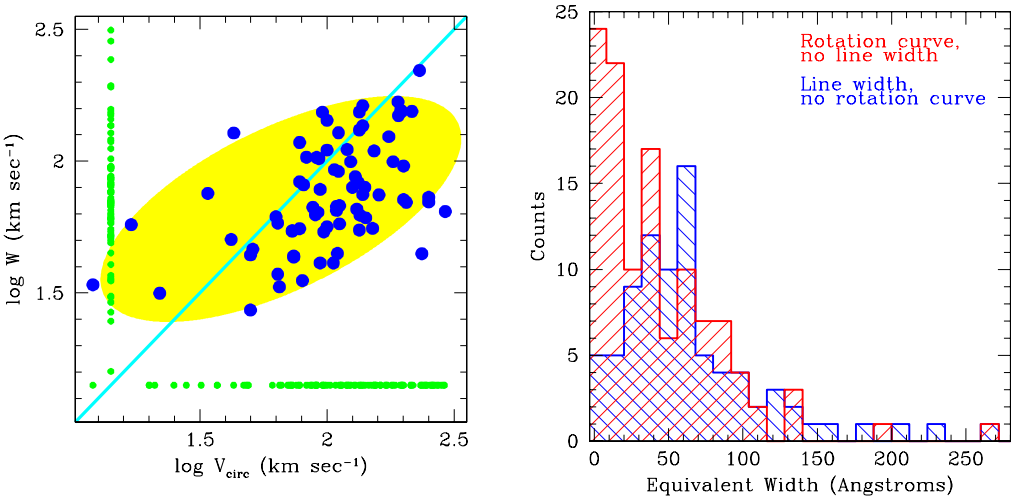

Figure 2. Left: the relationship between circular velocity and integrated velocity width for emission line objects within the DEEP GSS general redshift sample. The yellow ellipse traces the locus of the points, while the thin cyan line is a one-to-one relationship. The horizontal and vertical green lines of points demonstrate that there are both galaxies for which an integrated width can be determined but a circular velocity cannot be measured, and galaxies for which the reverse is true. Right: histograms showing the distribution of equivalent widths for galaxies with rotation curves but no line widths (low equivalent width peak) and the reverse (higher equivalent widths).

flux requirements of the integrated width measurement technique. In the second panel we note that these objects tend to have faint emission lines and low equivalent widths, and are thus the type of galaxies which at high redshifts tend to follow the local Tully-Fisher relation. Care must thus be taken when examining integrated width samples to account for the bias toward bright, compact objects with known to congregate at brighter magnitudes than those suggested by their masses.

Acknowledgements

This work was conducted under the auspices of the DEEP (Deep Extragalactic Evolutionary Probe) project, which was established through the Center for Particle Astrophysics. Funding was provided by NSF grant AST-0349155 to NPV through the Career Awards program, by NSF-0123690 via the ADVANCE-IT Program at NMSU, and by NASA grants GO-07883.01-96A and GO-10249.01A.

References

Bamford, S. P., Aragón-Salamanca, A., & Milvang-Jensen, B. 2006, *MNRAS* 366, 308
Böhm, A., *et al.* 2004, *A&A* 420, 97
Nakamura, O., Aragón-Salamanca, A., Milvang-Jensen, B., Arimoto, N., Ikuta, C., & Bamford, S. P. 2006, *MNRAS* 366, 144
Simard, L., *et al.* 1999, *ApJ* 519, 563
Vogt, N. P., *et al.* 1996, *ApJ* 479, L121
Vogt, N. P., *et al.* 1997, *ApJ* 465, L15
Vogt, N. P., *et al.* 2006, *ApJ* in preparation
Weiner, B. J., *et al.* 2006, *ApJ* in press
Ziegler, B. L., *et al.* 2002, *ApJ* 564, L69

Discussion

VERHEIJEN: How often do you observe declining rotation curves in the high redshift sample? How confident are you in measuring V_{flat} instead of V_{max}?

VOGT: It is extremely difficult to determine the underlying shapes of rotation curves at the highest redshifts in this sample, due to the fact that the spectrograph slitlets and the seeing disks are on the order of an arcsecond in size and the galaxies are not much larger. I have a new project underway to examine this very question, so please check back with me next year.

VAN DER HULST: How do you treat the uncertainty in inclination angle? Especially in the distant objects, inclination angles are hard to determine and may affect/bias the results.

VOGT: Uncertainties in inclination angle are modeled through the simulation process where we create a two-dimensional spectrum for comparison with the actual telescope data, and a non-trivial fraction of the errors associated with the fundamental galaxy parameters are based upon them. Note that the error in measuring the inclination angle is a function not only of redshift but of inclination angle itself, and is modeled accordingly. We are also lucky that an error in inclination angle tends to move a galaxy along the Tully-Fisher relation rather than perpendicular to it.

BUREAU: What are the properties of the local galaxies which do not follow the Tully-Fisher relation?

VOGT: The lowest redshift objects offset from the Tully-Fisher relation tend to be small disky galaxies, with high I-band surface brightness levels.

https://doi.org/10.1017/S1743921306004935 Published online by Cambridge University Press